**Naval Research Laboratory**

Washington, DC 20375-5000

Nov. 8, 1988

**NRL Report 9136**



# A Tutorial on Imaging

W. H. CARTER

*Space Systems Technology Department*
*Naval Center for Space Technology*

**August 24, 1988**

SECURITY CLASSIFICATION OF THIS PAGE

# REPORT DOCUMENTATION PAGE

Form Approved
OMB No. 0704-0188

| | |
|---|---|
| 1a. REPORT SECURITY CLASSIFICATION<br>UNCLASSIFIED | 1b. RESTRICTIVE MARKINGS |
| 2a. SECURITY CLASSIFICATION AUTHORITY | 3. DISTRIBUTION / AVAILABILITY OF REPORT<br>Approved for public release; distribution unlimited. |
| 2b. DECLASSIFICATION / DOWNGRADING SCHEDULE | |
| 4. PERFORMING ORGANIZATION REPORT NUMBER(S)<br>NRL Report 9136 | 5. MONITORING ORGANIZATION REPORT NUMBER(S) |
| 6a. NAME OF PERFORMING ORGANIZATION<br>Naval Research Laboratory<br>6b. OFFICE SYMBOL (*If applicable*)<br>Code 8304 | 7a. NAME OF MONITORING ORGANIZATION |
| 6c. ADDRESS (*City, State, and ZIP Code*)<br>4555 Overlook Avenue, SW<br>Washington, D.C. 20375-5000 | 7b. ADDRESS (*City, State, and ZIP Code*) |
| 8a. NAME OF FUNDING / SPONSORING ORGANIZATION<br>8b. OFFICE SYMBOL (*If applicable*) | 9. PROCUREMENT INSTRUMENT IDENTIFICATION NUMBER |
| 8c. ADDRESS (*City, State, and ZIP Code*)<br>Washington, DC 20362-5000 | 10. SOURCE OF FUNDING NUMBERS<br>PROGRAM ELEMENT NO: 61153N; PROJECT NO: RR01402; TASK NO: 41; WORK UNIT ACCESSION NO: |
| 11. TITLE (*Include Security Classification*)<br>A Tutorial on Imaging | |
| 12. PERSONAL AUTHOR(S)<br>Carter, W. H. | |
| 13a. TYPE OF REPORT<br>Final<br>13b. TIME COVERED<br>FROM Nov 87 TO Mar 88 | 14. DATE OF REPORT (*Year, Month, Day*)<br>1988 August 24<br>15. PAGE COUNT<br>14 |
| 16. SUPPLEMENTARY NOTATION | |

| 17. COSATI CODES | | | 18. SUBJECT TERMS (*Continue on reverse if necessary and identify by block number*) |
|---|---|---|---|
| FIELD | GROUP | SUB-GROUP | Coherent imaging; Holography; Electromagnetic radiation |
| | | | |
| | | | |

19. ABSTRACT (*Continue on reverse if necessary and identify by block number*)

This report describes several different imaging techniques, conditions for their validity, how they differ, and why they are not really as closely related as it might superficially appear.

An attempt has been made not to exceed a level of mathematical presentation suitable for an electrical engineer well trained in circuit theory but not familiar with the analysis of wave propagation.

| | |
|---|---|
| 20. DISTRIBUTION / AVAILABILITY OF ABSTRACT<br>☒ UNCLASSIFIED/UNLIMITED ☐ SAME AS RPT ☐ DTIC USERS | 21. ABSTRACT SECURITY CLASSIFICATION<br>UNCLASSIFIED |
| 22a. NAME OF RESPONSIBLE INDIVIDUAL<br>William H. Carter | 22b. TELEPHONE (*Include Area Code*)<br>(202) 767-2453<br>22c. OFFICE SYMBOL<br>Code 8304 |

DD Form 1473, JUN 86 *Previous editions are obsolete.* SECURITY CLASSIFICATION OF THIS PAGE

## CONTENTS

# A TUTORIAL ON IMAGING

## INTRODUCTION

Obtaining the coordinates of a military target in a weapons system computer, making an aerial photograph, mapping the terrain with side-looking radar, obtaining data for a terrain avoidance guidance system are all practical examples of imaging systems that use electromagnetic radiation. From the view point of the mathematical models we use to understand and compare such systems, they differ in detail but not in purpose. This report discusses various kinds of electromagnetic imaging systems of military interest, stressing their similarities and differences. This information should be useful to administrators who review and judge research proposals for developing military systems that use imaging devices of various kinds.

## COHERENT IMAGING

The easiest imaging systems to describe mathematically use coherent radiation like that from a laser or a radar transmitter. Because the propagation of coherent light can be easily described without the use of statistical models, we begin our discussion with coherent imaging.

### Coherent Imaging Through a Lens

Figure 1 shows a simple imaging system. Light from the source plane travels through a lens that forms an image of the light distribution from the source plane over the image plane. We assume that the light is coherent (i.e., strictly monochromatic) and also plane polarized. The light distribution over the source plane is described mathematically by the $x$-component of the electric field in that plane $E'(\mathbf{x}')$. Because Maxwell's equations, which describe the propagation of coherent light through dielectric media, are linear in the electric field amplitude, we may superimpose the responses of the lens to multiple source points in the source plane. Thus if a single source point at the position $\mathbf{x}'$ produces an image given by the spread function (i.e., impulse response) $h(\mathbf{x}, \mathbf{x}')$ in the image plane, the response to a distribution of source points in the source plane described by $E'(\mathbf{x}')$ is given by

$$E(\mathbf{x}) = \iint_{-\infty}^{\infty} E'(\mathbf{x}')\, h(\mathbf{x}, \mathbf{x}')\, d^2\mathbf{x}', \tag{1}$$

where $d^2\,\mathbf{x}' = dx'\,dy'$, a differential area within the source plane. In Eq. (1), $E$ and $E'$ are complex (phasor) functions of two spatial coordinates. Thus the actual time-dependent $x$-component of the electric field is given by the real part of

$$E(\mathbf{x}, t) = |E(\mathbf{x})|\, \exp\,(-i\omega t + i \arg\,(E(\mathbf{x}))). \tag{2}$$

If we assume that the response of the lens is spatially stationary so the $h\,(\mathbf{x}, \mathbf{x}') = h\,(\mathbf{x} - \mathbf{x}')$, we may take the two-dimensional Fourier transform of both sides of Eq. (1) to get

$$\tilde{E}(\boldsymbol{\xi}) = \tilde{E}'\,(\boldsymbol{\xi})\tilde{h}\,(\boldsymbol{\xi}), \tag{3}$$

where the tilde indicates the Fourier transform, viz.

Manuscript approved March 29, 1988.

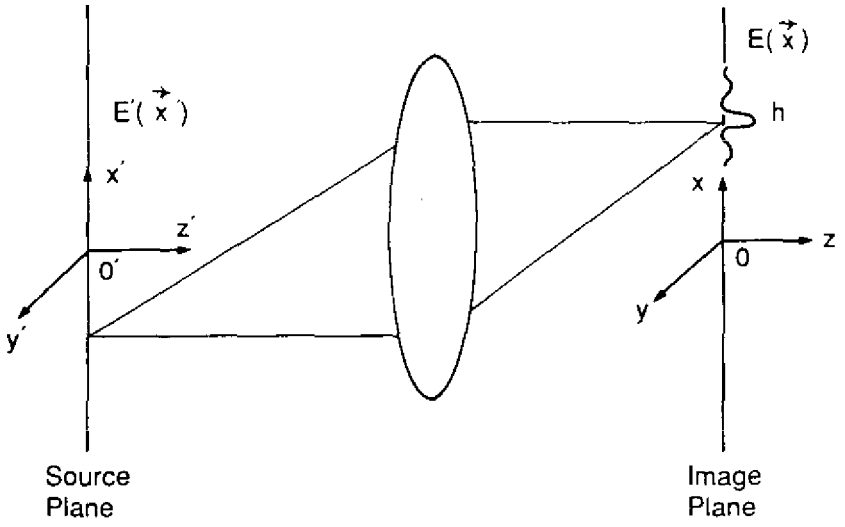


Fig. 1 — Coherent imaging through a lens

$$\tilde{E}(\xi) = \iint_{-\infty}^{\infty} E(\mathbf{x}) \exp(ik\mathbf{x} \cdot \xi)\, d^2\mathbf{x} \tag{4}$$

and $\tilde{h}$ is the complex transfer function for the lens. Thus the imaging properties of the lens are described mathematically by a complex transfer function, just like the mapping of a current or voltage through a two-port network in circuit theory. The major difference is that the lens system involves two spatial coordinates (and no causality) instead of one time coordinate (and causality).

## Coherent Imaging with Synthetic Aperture Radar

The operation of a synthetic aperture radar in its simplest form is mathematically identical to that of a lens. Instead of simply allowing the radiation to pass through the lens to focus in some image plane, with the radar the $x$-component of the electric field is actually sampled (in one dimension) by a radar receiver as the receiver is moved parallel to the $x'$ axis, as shown in Fig. 2. This data imperfectly represents the phasor describing the far-field radiation pattern of the radar target, i.e.,

$$\tilde{E}'(\xi) = \iint_{-\infty}^{\infty} E'(\mathbf{x}') \exp(ik\mathbf{x}' \cdot \xi)\, d^2\mathbf{x}'. \tag{5}$$

The effects of imperfect measurement and recording on the data can be simulated by multiplying $\tilde{E}'(\xi)$ by a transfer function $\tilde{h}(\xi)$. To obtain the one-dimensional image $E(\mathbf{x})$ ($x$-dependence only) in Fig. 2, the data must be inverse transformed by using a computer. Thus the imaging procedure is given by

$$\tilde{E}(\xi) = \tilde{E}'(\xi)\tilde{h}(\xi), \tag{6}$$

just as in Eq. (3) except that the image obtained is only one-dimensional (since our far-field data from the antenna can be measured only along the flight path in one dimension). In the radar model, $\tilde{h}$ represents the transfer function of the radar system caused by various imperfections in this procedure. To obtain the image in the direction parallel to the flight path, the data are recorded (corrupted by multiplication by the transfer function) and then inverse transformed to get the image. A second dimension perpendicular to the flight path is frequently added to the image by a completely different trick that is unique to radar. Remember that the sources are being illuminated by a radar transmitter

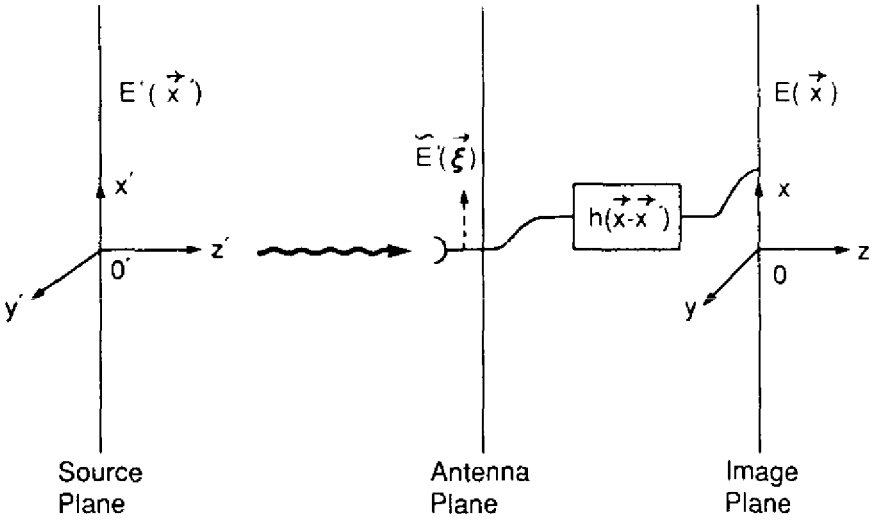


Fig. 2 — Synthetic aperture radar imaging

aboard the airplane carrying the receiver. The transmitter is designed to emit short pulses of radiation. Then a second image dimension perpendicular to the first, the range to the target from the airplane flight path, is measured by simply timing the flight of these pulses from the transmitter back to the receiver and multiplying by the speed of light. Synthetic aperture radar can also be made to work if the targets are not all in the far field of the antenna aperture; however, then the numerical methods required to refocus the data to form an image are slightly more complicated than a simple Fourier transform.

Note especially that the amplitude and the phase of the field at the antenna must be measured to obtain the image. Otherwise the complex phasor cannot be inverse transformed to obtain the image. If the radiation is not coherent, the phase is changing erratically during the measurement period and aperture synthesis in this way is not possible.

## Holography

Various holographic imaging techniques are very similar mathematically to synthetic aperture radar. (Holography in it's more modern form was invented by side-looking radar people at Willow Run Laboratories of the University of Michigan.) In holography, the amplitude and phase of the incident electric field are recorded as an interference pattern (using a mutually coherent reference wavefront) over the surface of a photographic plate. When the plate is properly processed and illuminated again with a backward-propagating replica of the reference wavefront, the complex conjugate of the recorded wavefront is reproduced. It then propagates backward to the original source plane to reconstruct an image of the source distribution (the source plane need not be in the far field of the hologram). The recording of the complex field data in the hologram is exactly analogous mathematically to the recording of the field by the radar receiver. The backward propagation of the conjugated field, upon reconstruction, is analogous to the inverse Fourier transformation of the radar data by computer. The radar data can also be processed by using it to make a computer-generated artificial hologram that will reconstruct an image in light of the radar targets. We stress again that the original target illumination must be coherent so that there is measurable phase data for the required phasors.

### An Important Property of Coherent Imaging

An image formed with coherent radiation looks different in some fundamental ways from the images we are used to seeing with conventional thermal light. With coherent light, the spread function in Eq. (1) gets bigger as the image is defocused so that the spread functions from different source points overlap in the image. Because the radiation is coherent, these overlapping spread functions interfere to produce a complicated diffraction pattern. As defocus is increased, the diffraction pattern changes but does not blur. Thus images of three-dimensional objects in coherent light are very noisy; this is caused by the diffraction patterns from out-of-focus portions of the image. This property of coherent images was first brought home to me in a vivid manner when as a graduate student I began working with my first home-made laser—using it to illuminate specimens under a microscope (see Carter, 1966, Ref. 1). Figure 3 (taken from Ref. 1 shows) a sequence of images of sugar crystals under a microscope as the image is defocused. The images to the right use conventional thermal illumination, and therefore, as the images become defocused they blur. The images to the left use laser illumination; as they become defocused by the same amounts as those on the right, they do not blur but instead break up into diffraction patterns. This is a basic problem with coherent images, no matter if they are formed by using radar at radio frequencies or by using lasers at light frequencies. Images made with coherent light are generally very noisy.

## INCOHERENT IMAGING

The most familiar imaging system for us is our eyes. Our eyes can detect only the intensity of the light at each point on our retina. Intensity is a measure of the power carried to that point at the retina by the light fields. The intensity for a single monochromatic, plane polarized component of thermal light is defined as a function of our field phasor by

$$I(\mathbf{x}) = \langle E^*(\mathbf{x})\, E(\mathbf{x}) \rangle , \tag{7}$$

where the sharp brackets denote an ensemble average. The ensemble average is essential for describing observations made with thermal light because of its stochastic nature. Unlike coherent radiation, thermal radiation does not yield measurable phasor field amplitudes like $E(\mathbf{x})$. The actual field amplitudes exist instantaneously, but the field amplitude fluctuates much too rapidly in both amplitude and phase to be measured because of the erratic nature of radiant heat (which is, of course, what thermal radiation is). Thus we treat the phasor $E(\mathbf{x})$ as a random variable that can be characterized by an ensemble of possible realizations. We assume that the statistics describing this random variable are ergodic, so the time averages that we must make to detect intensity are equal to the ensemble average defined in Eq. (7). Thus $I(\mathbf{x})$ in Eq. (7) is what we see.

It is easy to show that the intensity propagates linearly for thermal light. Consider thermal radiation from the source plane in Fig. 4 passing through a lens to form an image of the source distribution over the image plane. For a sufficiently short interval of time the electric field does not have time to fluctuate; thus the mathematical relations describing image formation are the same as those for coherent light in Eqs. (1) and (3). However, if we try to measure this field amplitude it is found to change during the period of measurement so that we will measure zero electric field (the average value of a fluctuating sinusoidal monochromatic field component). However, we can measure power (which has a nonzero average value). Thus multiplying Eq. (1) by its complex conjugate and taking the ensemble average we get

$$I(\mathbf{x}_i) = \int_{-\infty}^{\infty}\int_{-\infty}^{\infty} \langle E^*(\mathbf{x}_1')\, E(\mathbf{x}_2') \rangle\, h^*(\mathbf{x}_i, \mathbf{x}_1')\, h(\mathbf{x}_i, \mathbf{x}_2')\, d^2\mathbf{x}_1'\, d^2\mathbf{x}_2'. \tag{8}$$

Photomicrograph Magnification = 300

FOCUSED

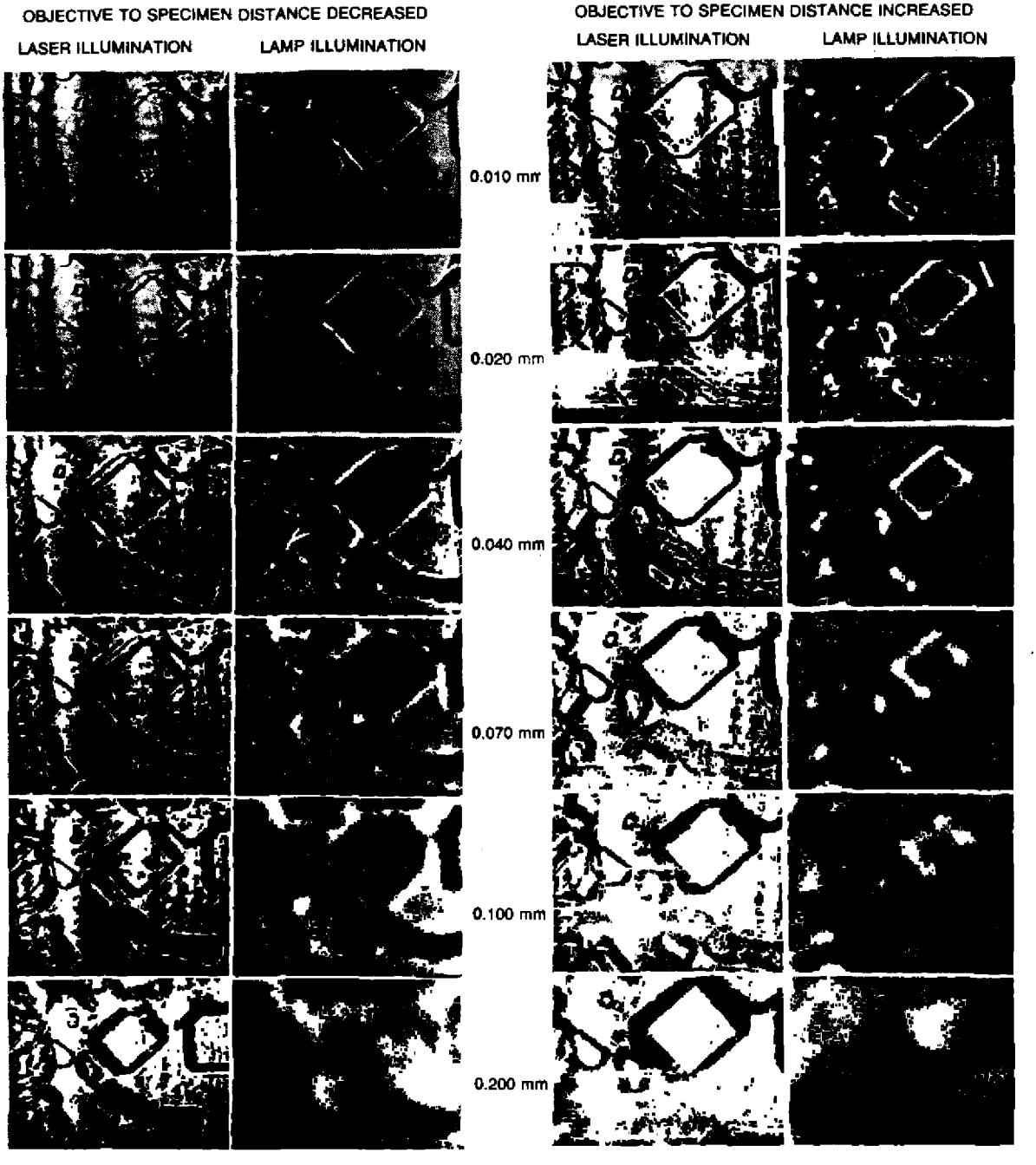


Fig. 3 — **Defocusing in a microscope** with both coherent laser illuminated images and thermally illuminated images

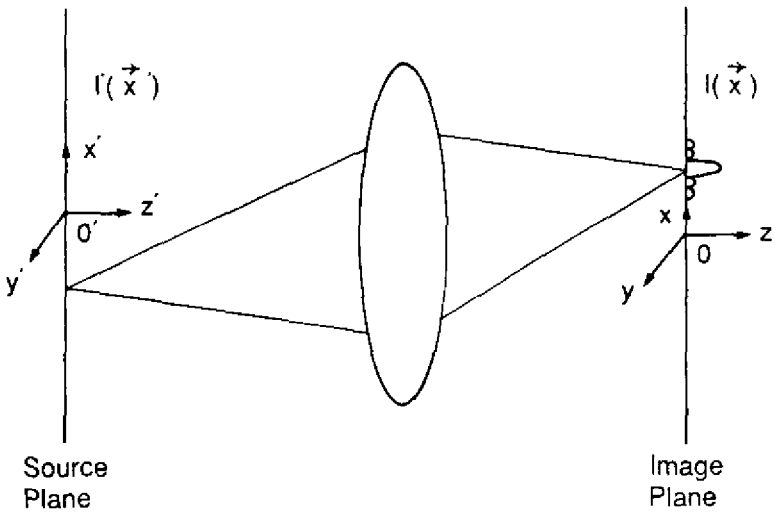


Fig. 4 — Incoherent imaging through a lens

If we assume that the radiation over the source plane is incoherent so that

$$<E^*(\mathbf{x}_1')\ E(\mathbf{x}_2') > \ = I(\mathbf{x}_1')\,\delta^2(\mathbf{x}_1' - \mathbf{x}_2'), \tag{9}$$

where $\delta^2$ is the two-dimensional Dirac delta function; upon substitution from Eq. (9) into Eq. (8) we have

$$I(\mathbf{x}) = \iint_{-\infty}^{\infty} I(\mathbf{x}')\,H(\mathbf{x}, \mathbf{x}')\,d^2\mathbf{x}', \tag{10}$$

where the incoherent spread function is given by

$$H(\mathbf{x}, \mathbf{x}') = |h(\mathbf{x}, \mathbf{x}')|^2. \tag{11}$$

We see that Eq. (10), which describes imaging with incoherent light, is somewhat similar, superficially, to Eq. (1), which describes image formation with coherent light. However, there are some important differences, as we saw from the data in Fig. 3. For one thing, the spread function in Eq. (1) is complex (since E is complex), whereas that in Eq. (10) is real (since $I$ is real). Thus defocusing provides phase-dependent interference effects only for coherent radiation. This is very fortunate because it allows reasonably noise-free vision with thermal light, uncluttered with diffraction patterns from out-of-focus detail. The second thing to notice is that coherent imaging, unlike thermal imaging, is nonlinear in the observable intensity. This means that the slightly overlapping images of nearby objects will interfere in a phase-dependent manner. Of course, cameras, telescopes, microscopes, and all lens systems which image with thermal light are mathematically the same as our eyes.

We have discussed coherent imaging and incoherent imaging with thermal light. Because of assumptions that we were able to make about these phenomena, the mathematical models that we can use to understand them are rather simple. However, we are still left with systems such as the radio telescope and the Naval Ocean Systems Center (NOSC) interferometer for which these assumptions fail. These systems are somewhat more complicated to understand mathematically. To do this, a relatively new system of mathematical models has been developed which is called the theory of partial coherence. The theory of partial coherence is still a specialized field in optics that is not well understood by most workers. In the last part of this tutorial, I will present just enough of this theory to allow its use in making clearer the unique properties of partially coherent imaging.

## PARTIALLY COHERENT IMAGING

How do we treat radiation problems for which the electric field fluctuates during intensity measurement—but not so rapidly or so greatly that all interference effects are averaged away? The theory must describe the observable interference effects but should also describe the extent to which interference effects are washed away. It should accurately describe just what we see. Such a theory has been developed largely as a result of the efforts of E. Wolf at the University of Rochester [2]. The observable parameter is taken to be the cross-spectral density function defined in terms of the $x$-component of the electric field vector for a monochromatic component of any radiation field by

$$W(\mathbf{x}_1, \mathbf{x}_2) = < E^*(\mathbf{x}_1)\, E(\mathbf{x}_2) >, \tag{12}$$

where the sharp brackets again denote an ensemble average and $E(\mathbf{x})$ is treated as a random variable. We note that the cross-spectral density function gives the intensity directly simply by setting $\mathbf{x}_1 = \mathbf{x}_2$. We also note that a radio telescope which measures the correlation function of the field amplitude between the electric field at one antenna at $\mathbf{x}_1$ and the electric field at a second antenna at $\mathbf{x}_2$ is measuring $W(\mathbf{x}_1, \mathbf{x}_2)$. Substituting Eq. (1) and its complex conjugate into Eq. (12) and then using Eq. (12) to define the cross-spectral density function in the kernel of the integral, we find that the cross-spectral density function propagates according to

$$W(\mathbf{x}_1, \mathbf{x}_2) = \int_{-\infty}^{\infty}\int_{-\infty}^{\infty} W(\mathbf{x}_1', \mathbf{x}_2')h^*(\mathbf{x}_1, \mathbf{x}_1')h\ (\mathbf{x}_2, \mathbf{x}_2')\, d^2\mathbf{x}_1'\, d^2\mathbf{x}_2'. \tag{13}$$

We recognize this as a simple extension of the superposition principal in Eq. (1) to four space dimensions. Thus for partially coherent light, the cross-spectral density function propagates linearly according to our superposition model.

### A Classic Radio Telescope

For a radio telescope, we assume that the radiation over the source plane as shown in Fig. 5 is thermal so that we have

$$W(\mathbf{x}_1', \mathbf{x}_2') = I(\mathbf{x}_1')\, \delta^2(\mathbf{x}_1' - \mathbf{x}_2'), \tag{14}$$

where $\delta^2$ is the two-dimensional Dirac delta function. We also assume that the cross-spectral density function is measured by a radio interferometer in the $\xi$ plane, which is in the far field of the source plane. The spread function in Eq. (11) is well known from antenna theory to be the Fourier kernel

$$h(\xi, \mathbf{x}') = \exp(ik\mathbf{x}' \cdot \xi). \tag{15}$$

Substituting from Eqs. (14) and (15) into Eq. (13) we find that the cross-spectral density function that we measure in the antenna plane is given by

$$W(\xi_1, \xi_2) = \int_{-\infty}^{\infty} I(\mathbf{x}') \exp(ik\mathbf{x}' \cdot (\xi_2 - \xi_1))\, d^2\mathbf{x}'. \tag{16}$$

Equation (16) says that the correlation function in its dependence on the separation of the two measuring antennas is the two-dimensional Fourier transform of the source intensity distribution for this incoherent source. Relations of this type are statements of the van Cittert Zernike theorem. We note immediately from Eq. (16) that the radiation, which was incoherent over the source plane, has gained

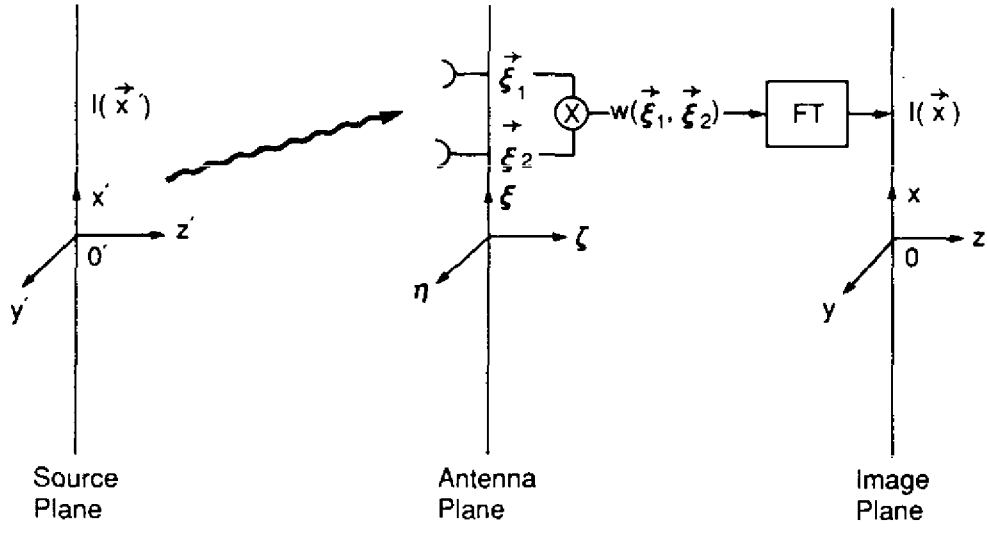


Fig. 5 — Imaging with a radio telescope

coherence as it propagates to our antenna plane. The field at our antennas is now partially coherent so that we measure the nonzero correlation function between antennas given by Eq. (16). This partial coherence is precisely what we use to form our image. It is clear from Eq. (16) that to form an image of the source distribution we need only invert the Fourier transform to get

$$I(\mathbf{x}) = \iint_{-\infty}^{\infty} W(\xi_1, \xi_2) \exp\left(-ik(\xi_2 - \xi_1) \cdot \mathbf{x}\right) d^2(\xi_2 - \xi_1). \tag{17}$$

Thus the imaging procedure for a classic radio telescope as described by Eq. (17) is theoretically straightforward.

## The NOSC Interferometer

The NOSC interferometer works quite differently than a radio telescope. For the NOSC approach, the cross-spectral density function is measured with a fixed antenna spacing $d$. The pair of antennas are moved together aboard an airplane flying along a path that is parallel to the source plane, as shown in Fig. 6. The presence of a radio source is detected, and the source is located by computer pattern recognition of characteristic patterns in the cross-spectral density data collected along the flight path as a function of airplane position. Since the cross-spectral density function in the far field of a planar incoherent source distribution as given by Eq. (16) is only a function of the separation of the two antennas, the measured data will always be constant if $d$ is held constant; there will be no pattern to use to locate the radio sources. Thus this imaging technique will not work unless the flight path is long enough that the source plane is within the near field of the line along which this data is collected (i.e., the aperture of the antenna array). We again assume that the radiation in the source plane is incoherent (as given by Eq. (14)). However, because we can no longer make the far-field approximation given in Eq. (15), the spread function is no longer the Fourier kernel. As a result, the measured cross-spectral density function is given by the NOSC interferometer by the expression

$$W(\xi_1, \xi_2) = \iint_{-\infty}^{\infty} I(\mathbf{x}')\, h^*(\xi_1, \mathbf{x}') h(\xi_2, \mathbf{x}')\, d^2\mathbf{x}'. \tag{18}$$

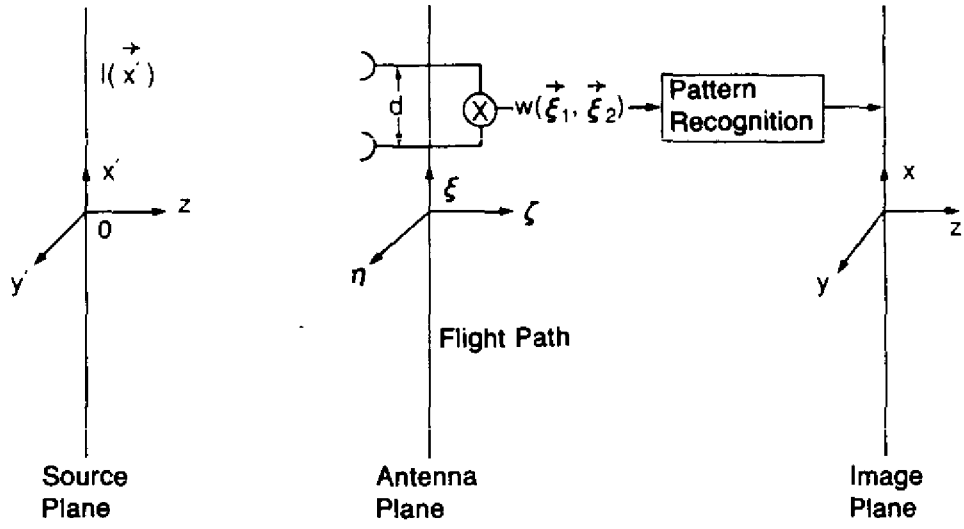


Fig. 6 — Imaging with the NOSC interferometer

Since $h^*(\xi_1, \mathbf{x}')h(\xi_2, \mathbf{x}')$ generally does not have an inverse like a Fourier kernel, Eq. (18) generally cannot be inverted to obtain the image. However, as NOSC engineers have pointed out, if the source plane is empty except for a few point sources, the presence of the $h^*(\xi_1, \mathbf{x}')h(\xi_2, \mathbf{x}')$ from a target can be detected in the measured cross-spectral density data by use of simple pattern recognition by a computer. From the detailed behavior of $h^*(\xi_1, \mathbf{x}')h(\xi_2, \mathbf{x}')$ and its location in the data, the target could be located. This will not work if there are so many sources that the spread functions in the data are heavily overlapping and cannot be identified and analyzed by the computer. The NOSC technique is not a general imaging technique that is applicable to continuous-tone objects like that used by radio astronomers. Rather, it is a specialized technique that might work if there are only a limited number of mutually incoherent point sources.

## CONCLUSIONS

As we have seen, parameters like the coherence of the radiation and approximations such as a far-field approximation make big differences in our ability to image and in the methods available to us to actually form that image. Many of the techniques involve Fourier transforms, spread functions, transfer functions, sampling data in an antenna plane, and the like, but this does not mean that all of the methods are essentially disguised versions of the the same thing. We cannot simply choose which imaging technique we want to use. These techniques are all very different, and their applicability frequently depends critically on conditions over which we do not always have control, as summarized in Table 1. The fact that the theories describing these imaging methods appear closely related has more to do with the extreme power of Fourier superposition models to deal with phenomena that are described by linear partial differential equations than to any similarity between the actual imaging methods. In my experience, attempts by sales engineers to equate different techniques sometimes reflects a lack of detailed understanding and can lead to confusion among their customers.

## REFERENCES

1. W. H. Carter, "Methods and Characteristics of Gas Laser Illumination in Microscopy," Ph.d. dissertation, Univ. Texas Austin (University Microfilms, Ann Arbor, Michigan, 1966).

2. M. Born and E. Wolf, *Principles of Optics* (Pergamon Press, New York, 1970), 4th ed.

Table 1 — Summary of Imaging Methods

| | **Coherent Imaging** | **Incoherent Imaging** | **Partially Coherent Imaging** |
|---|---|---|---|
| Linear Parameter | Field amplitude | Intensity | Cross-spectral density |
| Characteristics | Nonlinear in intensity | Linear in intensity | Generally *nonlinear* in intensity |
| | Noisy | Low noise | |
| | Can measure phase | Cannot measure phase | |
| Examples | Side-looking radar<br>Aperture synthesis<br>Holography<br>Inverse scattering<br>X-ray diffraction | Human vision<br>Cameras<br>Microscopes<br>Telescopes | Radio astronomy<br>NOSC method |
| Essential Requirements | Coherent Light<br>Phasor amplitude available | Incoherent light<br>Only intensity measured | Interferometer required |